Journal of Alloys and Compounds 509 (2011) 4304–4307

Contents lists available at ScienceDirect

Journal of Alloys and Compounds

journal homepage: www.elsevier.com/locate/jallcom

Investigation on the enhancement and the suppression of persistent luminescence of Re^{3+} doped $Sr_2EuMgSi_2O_7$ (Re = Dy, Yb)

Haoyi Wu, Yihua Hu*, Li Chen, Xiaojuan Wang

School of Physics and Optoelectronic Engineering, Guangdong University of Technology, Guangzhou 510006, PR China

ARTICLE INFO

Article history:
Received 4 September 2010
Received in revised form 5 January 2011
Accepted 7 January 2011
Available online 14 January 2011

Keywords:
Persistent luminescence
Thermoluminescence
Charge carriers transfer

ABSTRACT

The enhancement and the suppression of persistent luminescence on $Sr_2EuMgSi_2O_7$ are investigated by Dy^{3+} or Yb^{3+} doping. The TL curves show the deep traps induced by Yb^{3+} besides the intrinsic traps. The TL intensity of deep traps is stable whereas it decreases with preheating, indicating a charge carriers transfer process from the intrinsic traps to the deep ones. The mean lifetime of charge carriers in the deep traps is longer because of greater activation energy, restraining the detrapping. The similar process dominates the Dy^{3+} doped sample with an optimum trap depth, resulting in the enhancement of persistence luminescence.

1. Introduction

Persistent luminescence (long afterglow) has been known about for hundreds of years. Since the light emission persists for a long duration after stopping excitation, materials with this phenomenon have been used widely, such as the luminous paints, emergency signs, decoration, among others [1,2]. These materials are drawing more attention and the persistent luminescence has been achieved in many new kinds of materials, i.e. Tb^{3+} doped $CaZnGe_2O_6$ [3], Eu^{2+} and Re (Re: Rare earth) codoped $Ba_2ZnSi_2O_7$ [4], zinc–boron-germanosilicate glass–ceramics [5]. All these reveal the considerable potential applications of persistent luminescence materials. The conventional phosphors with persistent luminescence are the sulphides doped with copper, which are chemically unstable. The rare earth doped aluminates and silicates were reported as a new kind of persistent luminescent materials about one decade ago [6,7]. After that, more attention has been devoted studying these materials. It is generally believed that the persistent luminescence of materials involves luminescence centers and trap centers. Charge carriers are generated by the excitation in the luminescence centers and then trapped in the trap centers subsequently. Their detrapping is thermally activated, which can cause a delay in the spectral emission, causing the persistent luminescence [8]. Although this schematic diagram is agreed well, many aspects of the mechanism, such as the formation of the traps, the type of the trapped carriers (electrons or/and holes), the dynamics of the trapping and detrapping process, etc., still remain unclear.

The Eu^{2+} doped aluminates have already demonstrated the persistent luminescence. The addition of Dy^{3+} in case of $SrAl_2O_4$ or of Nd^{3+} in case of $CaAl_2O_4$ significantly increases the duration of the phosphorescence [9]. On the other hand, Dy^{3+} or Nd^{3+} also increases the phosphorescent duration of the Eu^{2+} activated $Sr_2MgSi_2O_7$ [10,11]. The earliest model for the generation of persistent luminescence came from Matsuzawa et al. [12]. After the $4f^7 \rightarrow 4f^65d^1$ excitation of the Eu^{2+}, holes were considered to be released to the valence band and trapped by Dy^{3+}/Nd^{3+}, leading to the Eu^+ and Dy^{4+}/Nd^{4+}. However, the formation of Eu^+ and Dy^{4+}/Nd^{4+} was found unacceptable [13,14], and it could not explain the persistent luminescence in the Eu^{2+} single doped phosphors either. Later, a new mechanism model based on the electron traps was proposed by Dorenbos [15,16]. According to his model, electrons were generated by excitation and trapped by Dy^{3+} through the conduction band. This model was developed by Aitasalo et al. [17], combining with the cation vacancies and the oxygen vacancies. The cation vacancies were introduced due to the charge compensation and they were regarded as the hole traps. On the other hand, oxygen vacancies, introduced because of the reducing atmosphere, were regarded as electron traps. Besides, cation vacancies aggregated with the oxygen vacancies and the Dy^{3+}/Nd^{3+}. After the excitation, photoionization of the electrons from Eu^{2+} to conduction band occurred followed by the electrons trapping to the oxygen vacancies and then the migration of the electrons from vacancies to Dy^{3+}/Nd^{3+} formed the Dy^{2+}/Nd^{2+} (or $Dy^{3+}/Nd^{3+} + e^-$). The reverse process of the release of the electrons from traps to Eu^{2+} produced the persistent luminescence. More recently, Wang et al. [18,19] studied the defect states of the Eu^{2+} and Nd^{3+} codoped $CaAl_2O_4$ persistent luminescence material. The complex clusters consisting of a Ca^{2+} vacancy and two Nd^{3+} ions were proposed. Some isolated Ca^{2+}

* Corresponding author. Tel.: +86 020 39322262; fax: +86 020 39322265.
E-mail address: huyh@gdut.edu.cn (Y. Hu).

0925-8388/$ – see front matter © 2011 Elsevier B.V. All rights reserved.
doi:10.1016/j.jallcom.2011.01.051

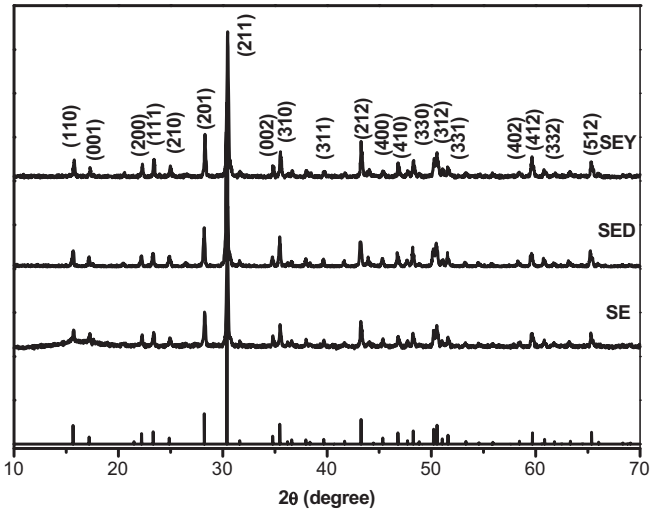

Fig. 1. The XRD patterns of the samples.

vacancies might act as bridges to transport charge carriers between trapping centers and emission centers. Models of both Aitasalo and Wang involved charge carriers transfer process and these models could explain the persistent luminescence in the Eu^{2+} single doped phosphors. Contrary to the Dy^{3+}/Nd^{3+}, Sm^{3+} or Yb^{3+} were reported to suppress the persistent luminescence in the Eu^{2+} doped $CaAl_2O_4$ and $Sr_2MgSi_2O_7$ matrices due to the removal of the cation vacancies caused by the reduction of Sm^{3+} or Yb^{3+} to Sm^{2+} or Yb^{2+} [20,21]. In the present work, the comparison of enhancement and suppression of the persistent luminescent properties in $Sr_{1.99}Eu_{0.01}MgSi_2O_7$ is studied by Dy^{3+} and Yb^{3+} codoping, respectively. Details of the thermoluminescence (TL) present the new deep traps induced by Yb^{3+} doping and charge carriers transfer process from the shallow traps to the deep ones. These explain the suppression of the luminescent properties with Yb^{3+} doping and it may assist to develop the mechanism of the persistent luminescence.

2. Experimental procedures

The phosphors $Sr_{1.99}Eu_{0.01}MgSi_2O_7$ (denoted as SE), $Sr_{1.97}Eu_{0.01}Dy_{0.02}MgSi_2O_7$ (denoted as SED) and $Sr_{1.97}Eu_{0.01}Yb_{0.02}MgSi_2O_7$ (denoted as SEY) were synthesized via the high temperature solid-state reaction with $SrCO_3$, MgO, SiO_2, Eu_2O_3, Dy_2O_3 and Yb_2O_3 as the raw materials. Additionally 8 mol% H_3BO_3 was added as a flux. All raw materials were analytically pure. After milling thoroughly, the mixtures were sintered at 1250 °C for 2 h in a weak reducing atmosphere (95%N_2 + 5%H_2). The phase and the structural purity of the samples were verified by powder X-ray diffraction (XRD). The photoluminescence of the samples was studied by using a Hitachi F-7000 fluorescence spectrophotometer. The decay curves and the TL curves of the samples were recorded with a FJ-427A1 thermoluminescent dosimeter. Prior to the measurement of the decay curves, the samples were exposed under a fluorescent lamp (the wavelength is from UV to red, 9 W) for 1 min. Before the measurement of each TL curve, the samples were also excited by a fluorescent lamp for 1 min. The heating rate for TL is 1 K s^{-1}.

3. Results and discussion

The XRD analysis of the samples was carried out. As shown in Fig. 1, the phases of SE, SED and SEY can be indexed to the tetragonal structure of $Sr_2MgSi_2O_7$ in the space group $P\text{-}42_1m$ (No. 113) according to the JCPDS standard card No. 75-1736. The cell parameters are $a = b = 7.995$ Å and $c = 5.152$ Å. No other structure is observed. The Eu^{2+} (coordination no. = 8, radius: 125 pm), Dy^{3+} (coordination no. = 8, radius: 103 pm) and Yb^{3+} (coordination no. = 8, radius: 99 pm) tend to substitute the Sr^{2+} (coordination no. = 8, radius: 126 pm) in the matrix because of the approximate ionic size. The Mg^{2+} (coordination no. = 4, radius: 57 pm) and Si^{4+} (coordination no. = 4, radius: 26 pm) are too small to be replaced.

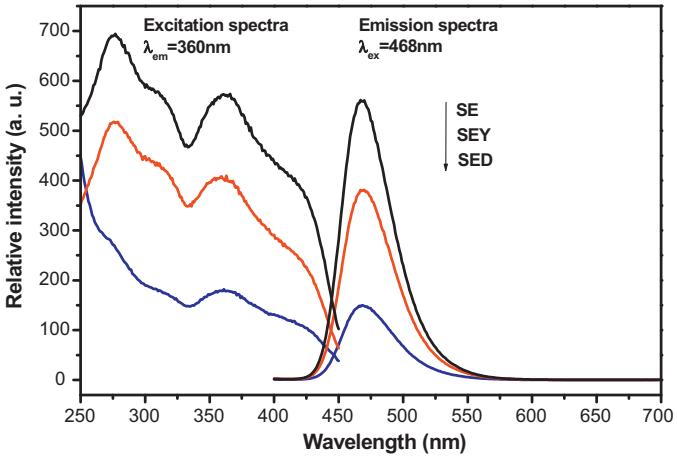

Fig. 2. The excitation and emission spectra of the samples.

The excitation spectra and the emission spectra are shown in Fig. 2. All samples exhibit a broad emission band centering on 468 nm under 360 nm excitation. Two broad absorption bands peaking at about 270 nm and 360 nm respectively are observed within the range of 250 nm to 450 nm. These spectra correspond to the excited state ($4f^65d^1$) to the ground state ($4f^7$) transition of the Eu^{2+} ions. The emission intensity of SEY is weaker than that of SE, indicating the suppression of the luminescent properties with Yb^{3+} doping. The emission intensity of SED is the weakest one, implying the lowest luminescent efficiency. The decay curves of the samples are shown in Fig. 3. On contrary, SED presents the strongest luminescent intensity, meanwhile, the intensity of SEY is also weaker than that of SE. The double exponential function is utilized to fit into the decay curves. The formation of the function is as follows:

$$I = I_1 \exp\left(\frac{-t}{\tau_1}\right) + I_2 \exp\left(\frac{-t}{\tau_2}\right) \quad (1)$$

where I is the phosphorescent intensity. I_1 and I_2 are constants. The parameters τ_1 and τ_2 imply the duration of persistent luminescence. The fitting results are shown in Table 1. A greater value of τ_2 reflects a longer duration of persistent luminescence. As indicated in the table, Dy^{3+} doping prolongs the duration whereas Yb^{3+} doping shortens the duration. These results illustrate the enhancement of Dy^{3+} and the suppression of Yb^{3+} on the persistent luminescent properties.

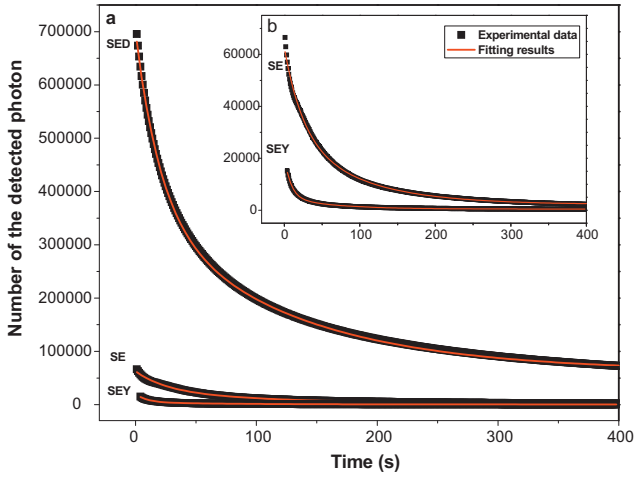

Fig. 3. (a) The decay curves of SE, SED and SEY; (b) the decay curves of SE and SEY.

Table 1
The fitting results of decay curves.

Samples	τ_1 (s)	τ_2 (s)
SE	24.2	91.4
SED	20.4	120.5
SEY	8.8	20.4

Table 2
The estimated results of μ_g of TL curves with preheating.

	Delay time						
	3 min	5 min	10 min	15 min	20 min	30 min	1 h
Value of μ_g	0.43	0.42	0.43	0.44	0.43	0.44	0.43

Since Yb^{3+} has one less electron than required for stable electronic configuration, it can be reduced to Yb^{2+} easily [20–22]. Therefore, the concentration of the cation vacancies will decrease because of the low probability of charge compensation. Afterwards, it is reasonable to believe that Dy^{3+} doping has better phosphorescent properties because of the unreduced Dy^{3+} ions. However, the sample with single Eu^{2+} doping shows a longer phosphorescent duration rather than Eu^{2+} and Yb^{3+} codoping. Consequently, concentration of the vacancies should not be the main reason because SE with less cation vacancies maintains the better phosphorescent properties (stronger initial intensity and longer phosphorescent duration). In order to provide a further explanation, the TL curves of the samples are investigated. Fig. 4 shows the TL curves of the samples with 15 min delay time (interval between excitation and the measurement). SE exhibits a single broad band peaking at about 78 °C. With Dy^{3+} doping, SED exhibits a much stronger TL band than SE. This band peaks at about 85 °C. On the other hand, SEY shows a comparable TL intensity but the shape is more complicated. Deconvolution of this TL is carried out and the results are shown in Fig. 4. Two TL bands which peak at 78 °C and 110 °C are obtained, respectively. It implies the new traps introduced by the Yb^{3+} doping, in addition to intrinsic traps in SE. These new traps are deeper than the intrinsic one because more activation energy is needed to release the trapped carriers. Afterwards, charge carriers transfer in these traps may occur. If this is the case, the suppression of the Yb^{3+} doping on the luminescent properties can be explained properly. The TL curves of SEY with various delay times are measured and shown in Fig. 5(a). As shown in the figure, two TL bands show different attenuations. The band responsible for the shallow

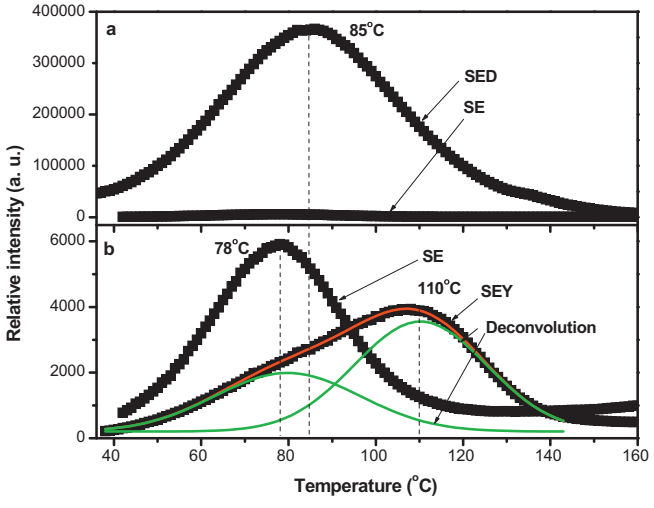

Fig. 4. (a) The TL curves of SE and SED; (b) the TL curves of SE and SEY with the fitting results.

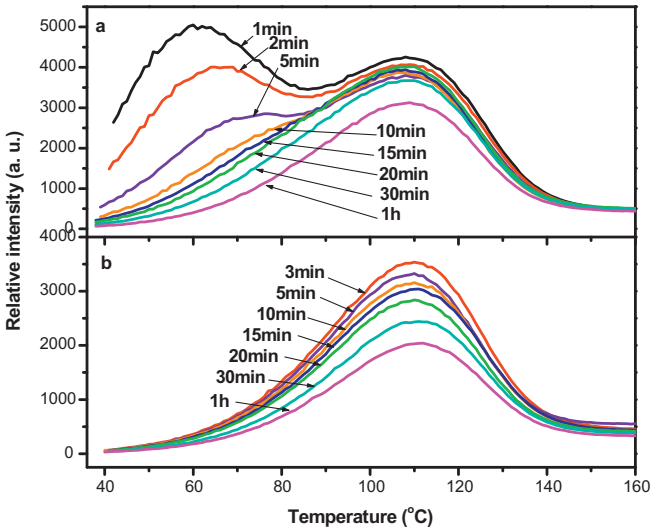

Fig. 5. (a) The TL curves of SEY with various delay times; (b) the TL curves of SEY with various delay times after the preheating process.

intrinsic traps has a rapid attenuation while the band responsible for the deep traps maintains a stable intensity unless the delay time reaches to 1 h. Since activation energy is greater, charge carriers should have a longer mean lifetime in deep traps. Therefore, their detrapping probability is relative low, implying that the traps have a very slow attenuation [23,24], or maybe do not have a significant attenuation. However, an obvious attenuation occurs from 30 min to 1 h delay time. The stable TL intensity may be due to the influence of the intrinsic traps. In order to avoid this influence, the TL curves of SEY were also measured with preheating from room temperature to 90 °C (heating rate: 1 K s^{-1}). The interval between the excitation and the preheating was 1 min. Then the TL curves were measured again. These curves are shown in Fig. 5(b). Instead of a stable intensity, the TL band decreases monotonically in this case. Since the intrinsic traps are almost bleached during preheating, it is reasonable to believe that this monotonically decrease originates from attenuation of the concentration of the charge carriers in the deep traps. Consequently, an explanation for the suppression of the luminescent properties with Yb^{3+} doping can be proposed. Lots of charge carriers are generated after excitation and they are trapped by the trapping centers subsequently. With Yb^{3+} doping, new traps with high activation energy are created, and it traps the charge carriers. This group of charge carriers is not easy to be detrapped at room temperature. Charge carriers in intrinsic traps partially transfer to the deep traps, so that the entire detrapping process declines. This leads to the suppression of the persistent luminescent properties. However, if the intrinsic traps are bleached or retain a small amount of trapped carriers, no transfer of the charge carriers occurs. That is why a decrease of TL band is obtained after 30 min or with a preheating process.

The transfer process of the trapped carriers still remains unclear. If the lattice defects corresponding to the intrinsic traps are further away from the defects corresponding to the Yb^{3+} codoping, charge carriers may be thermally released to the conduction/valence band and then retrapped by the deep traps. This conforms to Sun's work [25]. On the other hand, Sr^{2+} vacancies will attract the oxygen vacancies and the Yb^{3+} ions. Then electrons in the oxygen vacancies may be released to the vicinity of Yb^{3+} directly [17]. This is also the possible case since oxygen vacancies, which are induced via the reducing atmosphere during synthesis process, are probably the cause of the intrinsic traps. Chen [26,27] has studied the TL theoretically and he provides a method to identify the kinetic order for a model of one trap according to the shape of the TL band. The

method involves a parameter μ_g, which equals δ/ω. Here δ represents the half width toward the fall off of the glow peak and ω is the total half width of the band. The value of μ_g is 0.42 for the first order case and is 0.52 for the second order case. In the present work, μ_g for each TL curve with preheating is estimated and the results are listed in Table 2. The value of μ_g indicates that first order kinetics dominates the TL process of the deep traps. In addition, T_m (temperature corresponding to the maximum of TL) is a constant in the first order case while it shifts toward the high temperature direction with the decrease of the charge concentration in the second order case [24,28]. As shown in Fig. 5 (a), the glow peak responsible for intrinsic traps moves to higher temperature with the decrease of the concentration of the trapped carriers, confirming the second order case. Meanwhile, T_m in Fig. 5(b) gives a further evidence for the first order kinetics of the deep traps. Hence the probability of the retrapping of deep traps is low. Charge carriers in the intrinsic traps are thermally released to the deep traps which induced by Yb^{3+} ions directly. This dominates the charge carriers transfer process between the traps.

In the $Sr_2MgSi_2O_7$: Eu^{2+}, Yb^{3+} phosphors, some of the Yb^{3+} ions are reduced to Yb^{2+} ions and then some Sr^{2+} vacancies which act as hole traps are physically removed. On the other hand, Yb^{3+} ions provide deep traps, in which trapped carriers have longer lifetime. The transfer process from intrinsic traps to deep traps by the charge carriers decreases the detrapping. That is why the persistent luminescence is suppressed by Yb^{3+} doping. For the case of Dy^{3+}, the persistent luminescent properties are enhanced significantly. Since Dy^{3+} have 9 electrons in the f state (not close to the stable configuration of 14 electrons), it is difficult to be reduced to Dy^{2+}. Therefore many Sr^{2+} vacancies and Dy^{3+} defects are created. According to the model provided by Aitasalo et al. [17,29], both oxygen vacancy and Dy^{3+} act as electron traps and they are connected by a Sr^{2+} vacancy. The TL curves indicate that the depth of the traps induced by Dy^{3+} is very close to the intrinsic traps which are probably oxygen vacancies (maybe quasi-continuum). Then part of the electrons trapped by oxygen vacancies transfer to Dy^{3+}, forming Dy^{2+} or $Dy^{3+} + e^-$. The detrapping of electrons delays the emission then leads to the persistent luminescence [30]. On the other hand, the traps induced by Yb^{3+} are much deeper owing to the lower 4f energy level of Yb^{2+} [15]. Electrons in oxygen vacancies transfer to Yb^{3+}, Yb^{2+} or the $Yb^{3+} + e^-$ clusters which are more stable, restraining the detrapping. These are the reasons for the enhancement and the suppression of persistent luminescence, respectively. In addition, lots of Sr^{2+} vacancies exist in SED and they attract oxygen vacancies and Dy^{3+} ions. A short distance between these two defects may trap electrons more efficiently. That is why SED shows a low luminescent efficiency and much greater TL intensity than SE. It may be another reason for the enhancement of persistent luminescence.

4. Conclusions

As depicted in the present work, new traps are induced in addition to the intrinsic ones, by the introduction of Dy^{3+} or Yb^{3+} in Eu^{2+} doped $Sr_2MgSi_2O_7$. Then charge carriers in the intrinsic traps partially transfer to the deep ones. Depths of the traps result in two opposing effects on the luminescent properties. The traps induced by Yb^{3+} are too deep to detrap mass of charge carriers, hence the Yb^{3+} doping suppresses the persistent luminescence. Meanwhile, the traps induced by Dy^{3+} possess an optimum depth for detrapping, so the Dy^{3+} doping enhances the persistent luminescence.

Acknowledgements

The authors acknowledge the financial support from the National Natural Science Foundation of China (Nos. 21071034, 20871033). Dr. Robert Kelly in Guangdong University of Technology made a careful check of the language in this work.

References

[1] Y. Chen, X. Cheng, M. Liu, Z. Qi, C. Shi, J. Lumin. 129 (2009) 531–535.
[2] X. Teng, Y. Liu, Y. Liu, Y. Hu, H. He, W. Zhuang, J. Lumin. 130 (2010) 851–854.
[3] C. Liu, G. Che, Z. Xu, Q. Wang, J. Alloys Compd. 474 (2009) 250–253.
[4] S. Yao, Y. Li, L. Xue, Y. Yan, J. Alloys Compd. 410 (2010) 200–203.
[5] G. Lin, G. Dong, D. Tan, X. Liu, Q. Zhang, D. Chen, J. Qiu, Q. Zhao, Z. Xu, J. Alloys Compd. 504 (2010) 177–180.
[6] Y. Murayama, N. Takeuchi, Y. Aoki, T. Matsuzawa, U.S. Patent (13 June 1995) No. 5,424,006.
[7] Z. Xiao, Z. Xiao, U.S. Patent (25 July 2000) No. 6,093,346.
[8] F. Clabau, X. Rocquefelte, S. Jobic, P. Deniard, M.-H. Whangbo, A. Garcia, T. Le Mercier, Chem. Mater. 17 (2005) 3904–3912.
[9] H. Yamamoto, T. Matsuzawa, J. Lumin. 72–74 (1997) 287–289.
[10] A.A.S. Alvani, F. Moztarzadeh, A.A. Sarabi, J. Lumin. 115 (2005) 147–150.
[11] H. Wu, Y. Hu, Y. Wang, B. Zeng, Z. Mou, L. Deng, W. Xie, J. Alloys Compd. 486 (2009) 549–553.
[12] T. Matsuzawa, Y. Aoki, N. Takeuchi, Y. Murayama, J. Electrochem. Soc. 143 (1996) 2670–2673.
[13] T. Aitasalo, J. Hölsä, H. Jungner, M. Lastusaari, J. Niittykoski, J. Lumin. 94–95 (2001) 59–63.
[14] T. Aitasalo, P. Doreń, J. Hölsä, H. Jungner, J.-C. Crupa, M. Lastusaari, J. Lengendziewicz, J. Niittykoski, W. Strek, J. Solid State Chem. 171 (2003) 114–122.
[15] P. Dorenbos, Phys. Status Solidi (b) 242 (2005) R7–R9.
[16] P. Dorenbos, J. Electrochem. Soc. 152 (2005) H107–H110.
[17] T. Aitasalo, J. Hölsä, H. Jungner, M. Lastusaari, J. Niittykoski, J. Phys. Chem. B 110 (2006) 4589–4598.
[18] Y. Wang, L. Wang, J. Appl. Phys. 101 (2007) 53–108.
[19] L. Wang, Y. Wang, X. Xu, J. Appl. Phys. 104 (2008) 13519.
[20] T. Aitasalo, P. Dereń, J. Hölsä, H. Jungner, M. Lastusaari, J. Niittykoski, W. Strek, Radiat. Meas. 38 (2004) 515–518.
[21] A.A. Setlur, A.M. Srivastava, H.L. Pham, M.E. Hannah, U. Happek, J. Appl. Phys. 103 (2008) 53513.
[22] C.-H. Huang, Rare Earth Coordination Chemistry: Fundamental and Applications, Wiley-VCH, 2010.
[23] W. Drozdowski, D. Wisniewski, A.J. Wojtowicz, A. Lempicki, P. Dorenbos, J.T.M. de Haas, C.W.E. van Eijk, A.J.J. Bos, J. Lumin. 72–74 (1997) 756–758.
[24] R. Chen, S.W.S. McKeever, Theory of Thermoluminescence and Related Phenomena, World Scientific Published Co., Singapore, 1997.
[25] X. Sun, J. Zhang, X. Zhang, Y. Luo, Z. Hao, X.-j. Wang, J. Appl. Phys. 105 (2009) 013501.
[26] R. Chen, J. Electrochem. Soc. 116 (1969) 1254–1257.
[27] R. Chen, J. Appl. Phys. 40 (1969) 570–585.
[28] A.J.J. Bos, Radiat. Meas. 41 (2007) S45–S56.
[29] J. Hölsä, T. Laamanen, M. Latsusaari, M. Malkamäki, P. Novák, J. Lumin. 129 (2009) 1606–1609.
[30] H. Wu, Y. Hu, Y. Wang, C. Fu, J. Alloys Compd. 497 (2010) 330–335.